

Analysis of the Periodic Bursting Oscillations Induced by Different Non-Smooth Evolution Patterns

Weihong Mao*

Faculty of Science, Jiangsu University, Zhenjiang, Jiangsu 212013, P.R. China

(Received 31 December 2019, accepted 12 March 2020)

Abstract: The main purpose of this paper is to investigate bursting oscillations and the mechanism in a Filippov-type system with a slow-changing external excitation and a non-smooth boundary via a modified Chua's circuit model. Based on the idea of the slow-fast analysis method, equilibrium branches and the related bifurcations of the subsystems are obtained when regarding the external excitation as a slow-changing parameter, while the potential non-smooth evolutions in the non-smooth boundary are discussed via differential inclusion theory. Combined with numerical simulations, three different periodic bursting oscillations as well as the mechanism are studied. It shows that even similar equilibrium branch structures and identical bifurcation patterns can induce different bursting oscillations on account of the non-smooth evolutions. Furthermore, two different incentives to quiescent states can be found in the bursting oscillations, i.e., the sliding motion lying in the non-smooth boundary and the stable equilibrium branches located in smooth regions.

Keywords: Filippov-type system; non-smooth bursting oscillation; transformed phase portrait; non-smooth evolution; sliding motion

1 Introduction

In recent years, bursting phenomena have been interested by many researchers. Essentially, the order-gap of the changing rates between the variables in a dynamic system is the key to induce the bursting phenomena, which frequently may cause the trajectory to exhibit periodic oscillations with alternations between spiking states (SPs) and quiescent states (QSs). Such phenomena have been massively reported in experiments and mathematical models in neuroscience[1–3], physics[4, 5] and chemistry[6, 7].

A classic analysis method of dynamical evolution of bursting phenomena, named slow-fast analysis method, is introduced by Rinzel via dividing the whole dynamic system into two subsystems, i.e., the fast subsystem and the slow subsystem[8]. Based on this method, traditional bifurcation theory is applied by Izhikevich[9] to the two important bifurcations connecting the spiking states (SPs) and the quiescent states (QSs), which not only reveal the mechanism of transitions between SPs and QSs but also classify the bursting attractors. Particularly for non-autonomous systems, such as periodically excited systems, the method is very effective when an order gap exists between the external exciting frequency and the natural frequency. In the case that the exciting frequency is far less than the natural frequency, by regarding the whole exciting term as a slow-changing parameter, the so-called generalized autonomous system which can be considered as a fast subsystem is obtained. Moreover, the conception of transformed phase portrait (TPP)[10] is also introduced to successfully reveal the mechanism of bursting oscillations.

Up to now, the vector fields in the previous researches related to bursting oscillations are almost continuous, no matter what the relevant dynamic systems are autonomous or not[11–13]. In fact, many non-smooth properties such as dry friction in mechanical systems[14–16] and threshold effect in ecosystems[17–19] can cause the discontinuity of the vector fields, leading to that the bursting attractor structures may be more complex, which would be a new challenge to the mechanism as well as the classification of the bursting oscillations in such dynamic systems.

*E-mail address: 1000002878@ujs.edu.cn

In this paper, we mainly focus on the bursting oscillations in the systems with discontinuous vector fields (Filippov-type systems) by considering a modified Chua's circuit, in which a bilateral diode as well as a harmonically changed electrical source are introduced. The distinctive bursting attractor structures as well as the mechanism induced by non-smooth evolutions on the non-smooth boundary are studied.

The rest paper is organized as below. In section 2, a general introduction for the dynamical system is given. The analyses of equilibrium branches as well as the related bifurcations and the calculations of the potential non-smooth evolutions on the non-smooth boundary are both given in section 3. In the following section, three different bursting oscillations with special non-smooth behaviors corresponding to different parameter values are obtained by numerical simulations, from which the mechanism as well as the classification can be demonstrated on the basis of the analyses in section 3. The last section concludes this paper.

2 Mathematical model

Based on the canonical three-dimensional Chua's model[20], a non-autonomous Filippov-type dynamic system with a single non-smooth boundary as well as an exciting term via introducing a diode as well as a harmonically changed electrical source can be derived. The dimensionless form of the system can be expressed as:

$$\begin{cases} \dot{x} = y - x - (\alpha x + \beta x^3 + \gamma x^5) + A \sin(\Omega\tau) + \delta \operatorname{sgn}(x), \\ \dot{y} = x - y + z, \\ \dot{z} = -\eta y. \end{cases} \quad (1)$$

The non-smooth boundary $\Sigma : \{(x, y, z) | x = 0\}$ defined by $\delta \operatorname{sgn}(x)$ divides the vector field into two smooth regions, expressed by $D_+ = \{(x, y, z) | x > 0\}$ and $D_- = \{(x, y, z) | x < 0\}$ corresponding to the two non-autonomous smooth subsystems F_+ and F_- , respectively.

Fixing the frequency of the external excitation as $0 < \Omega \ll 1$, the external excitation may change on a much smaller scale than the one of the state variables in system (1). Thus, the whole external excitation can be regarded as a slow-changing parameter, denoted by w , leading to so-called generalized autonomous system.

3 Theoretical analysis

Since the whole external excitation $A \sin(\Omega\tau)$ can be regarded as a slow-changing parameter w , the generalized equilibrium points as well as the related bifurcations can be obtained, while the potential non-smooth evolutions when the trajectory comes into contact with the non-smooth boundary Σ can also be discussed by employing differential inclusion theory via introducing an auxiliary parameter.

3.1 Bifurcation analysis of the two subsystems

Note that the whole external excitation has been replaced by the slow-changing parameter w in the generalized autonomous system, the generalized equilibrium points of the two smooth subsystems can be expressed in the unified form $EQ = (x_0, 0, -x_0)$, where x_0 satisfies:

$$x_0 - (\alpha x_0 + \beta x_0^3 + \gamma x_0^5) + w + \delta \operatorname{sgn}(x_0) = 0. \quad (2)$$

The stability of which can be determined by the associated characteristic equation, expressed by:

$$\lambda^3 + h_1 \lambda^2 + h_2 \lambda + h_3 = 0, \quad (3)$$

where

$$\begin{cases} h_1 = \alpha + 2 + 3\beta x_0^2 + 5\gamma x_0^4, \\ h_2 = \alpha + \eta + 3\beta x_0^2 + 5\gamma x_0^4, \\ h_3 = \eta(\alpha + 1 + 3\beta x_0^2 + 5\gamma x_0^4). \end{cases} \quad (4)$$

Obviously, EQ is stable for $h_1 > 0, h_3 > 0$ and $h_1 h_2 - h_3 > 0$. There exist two ways by which EQ loses stability associated with two possible conventional bifurcations. One is the fold bifurcation, expressed by:

$$FB : h_3 = 0 (h_1 > 0, h_2 > 0), \quad (5)$$

meaning that the characteristic equation (3) appears single zero root. When the system crosses the criticality, one real eigenvalue may change from negative to positive, which may lead to jumping phenomena of the trajectory between different equilibrium points; while the other is the Hopf bifurcation, expressed by:

$$HB : h_1 h_2 - h_3 = 0 (h_1 > 0, h_2 > 0, h_3 > 0), \quad (6)$$

meaning that the characteristic equation (3) appears a pair of pure imaginary roots. When the system crosses the criticality, the real part of a pair of conjugate eigenvalues may change from negative to positive, which may lead to large amplitude motions of the trajectory. From (6) and (4), the necessary condition for the Hopf bifurcation frequency can be further calculated, expressed as:

$$\Omega_H^2 = h_2 = \eta - 1 \pm \sqrt{1 - \eta} > 0. \quad (7)$$

For simplicity and emphasizing the influence induced by the non-smooth evolutions in the potential bursting oscillations, the parameter is fixed as $\eta > 1$ in this paper, indicating that Hopf bifurcations is beyond the scope of this paper.

3.2 Non-smooth evolution analysis in the non-smooth boundary

The system (1) belongs to the family of Filippov-type systems. So, special non-smooth evolutions, such as sliding motion, may appear when the trajectory comes into contact with the non-smooth boundary Σ , which can be analyzed by employing differential inclusion theory[21] via introducing an auxiliary parameter q restricted in the continuously closed interval $[0, 1]$. The system (1), labeled by F , can be rewritten in the form:

$$F = qF_+ + (1 - q)F_-, \quad (8)$$

from which, the auxiliary parameter can be further calculated as the invariant form:

$$q = \frac{-y_s - w_s + \delta}{2\delta}, \quad (9)$$

in which, y_s and w_s are the values of the state variable y and the slow-changing parameter w of the trajectory when it comes into contact with the non-smooth boundary, respectively.

It is noted that three different ranges of the auxiliary parameter may exist, indicating that three different non-smooth evolutions may occur when the trajectory comes into contact with the non-smooth boundary. One is that the trajectory will behave sliding motion in the non-smooth boundary when the auxiliary parameter is located in the open interval $(0, 1)$; the second one is that the trajectory will pass through the non-smooth boundary from $D_- = \{(x, y, z) | x < 0\}$ to $D_+ = \{(x, y, z) | x > 0\}$ directly when the auxiliary parameter is located in $[1, +\infty)$; the last one is that the trajectory will switch to $D_- = \{(x, y, z) | x < 0\}$ from $D_+ = \{(x, y, z) | x > 0\}$ directly when the auxiliary parameter is located in $(-\infty, 0]$. Namely, when the auxiliary parameter breaks through the lower bound 0 of the interval $(0, 1)$, the system is governed by the subsystem F_- , while the auxiliary parameter breaks through the upper bound 1 of the interval $(0, 1)$, the system is governed by the subsystem F_+ .

4 Numerical simulations

Here, the parameters are fixed at $\alpha = 0.100, \gamma = 0.800, \eta = 1.100, \delta = -0.400, A = 1.200, \Omega = 0.005$. In the following, with different values of parameter β , we study the dynamics as well as the mechanism of the system involving two scales in frequency domain. Three different periodic bursting oscillations distinguished from different patterns the trajectory passes through the non-smooth boundary are obtained.

4.1 Non-smooth bursting oscillation with sliding-escaping motion

As shown in Fig1, one periodic bursting oscillation is obtained when the parameter is fixed at $\beta = -1.900$. In the phase portrait Fig1(a), it can be found that the trajectory enters into the non-smooth boundary Σ at the two points $P_{s1,2}$ and escapes from the non-smooth boundary at the point P_{s0} after it stays in Σ for a while. In a period of the oscillation, the trajectory can be divided into two parts by the non-smooth points located in the trajectory, one governed by the smooth subsystems F_{\pm} is located in the smooth regions D_{\pm} , including $P_{s0} \rightarrow P_{s1}$ and $P_{s0} \rightarrow P_{s2}$; the other is restricted in the non-smooth boundary behaving the obvious sliding motion, containing $P_{s1} \rightarrow P_{s0}$ and $P_{s2} \rightarrow P_{s0}$.

From the time history plotted in Fig1(b), the periodic bursting oscillation can exhibit four QS s and four SP s located in the two smooth regions D_{\pm} , denoted by $QS_{\pm i}(i = 1, 2)$ and $SP_{\pm i}(i = 1, 2)$, respectively, and two QS s restricted in the non-smooth boundary Σ , denoted by $QS_{s i}(i = 1, 2)$.

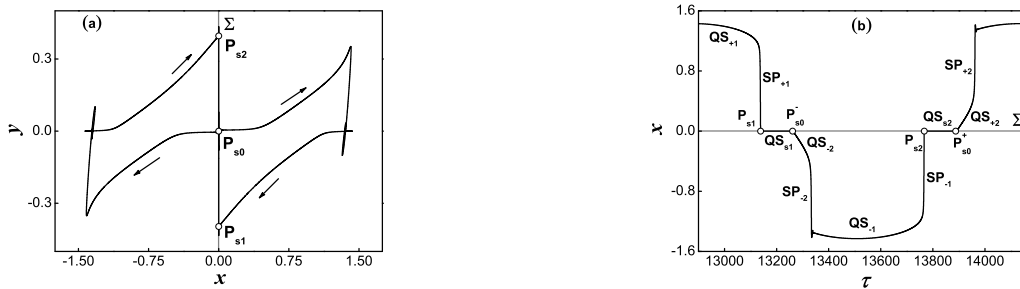


Figure 1: bursting oscillation with $\beta = -1.900$. (a) phase portrait; (b) time history.

To reveal the mechanism of such periodic bursting oscillation, Fig2(a) gives the equilibrium branches of the two generalized autonomous subsystems as well as the related bifurcations with the variation of the slow-changing parameter w , while the transformed phase portrait overlapped on the equilibrium branches as well as the related bifurcations is plotted in Fig2(b).

In the Fig2(a), the two equilibrium branches EB_{\pm} corresponding to the two subsystems can be separated into six segments (denoted by $EB_{\pm i}(i = 1, \dots, 6)$) by the four fold bifurcation points $FB_{\pm i}(i = 1, \dots, 4)$ and two connections points $N_{1,2}$ located in the non-smooth boundary, respectively, in which the two blue branches corresponding to the equilibria can be observed in the related subsystems, while the two red ones are not satisfied with the restriction of the non-smooth term any more. Meanwhile, the thinner branches denote the unstable solutions while the thicker ones denote the stable ones, respectively.

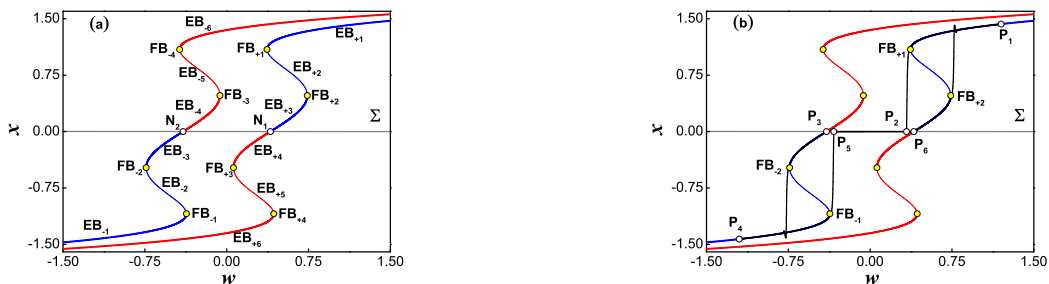


Figure 2: bursting oscillation with $\beta = -1.900$ (a) equilibrium branches of the two smooth subsystems; (b) overlap of the transformed phase portrait and the equilibrium branches.

The transformed phase portrait can be employed to investigate the mechanism of the periodic bursting oscillation. Without loss of generality, as shown in Fig2(b), assuming that the movement starts at the point P_1 with the maximum value of the external excitation, i.e., $w = +1.200$, the trajectory governed by the subsystem F_+ may strictly move along the stable focus-type equilibrium branch EB_{+1} with the increase of time τ , indicating that the system stays in

QS_{+1} . When the trajectory passes through the bifurcation point $FB_{+1}(w, x) = (0.3693, 1.0931)$, the stable focus-type equilibrium branch EB_{+1} meets the unstable equilibrium branch EB_{+2} and disappears together with EB_{+2} , i.e. fold bifurcation occurs, leading to that the trajectory may jump towards to the non-smooth boundary Σ and enter into the short spiking state SP_{+1} .

When the trajectory arrives at the point $P_2(w_2, x_2) = (0.3332, 0)$ located in the non-smooth boundary, corresponding to the point $P_{s1}(x_{s1}, y_{s1}) = (0, -0.3970)$ in the phase portrait Fig1(a), the auxiliary parameter may satisfy $q = \frac{-y_{s1} - w_2 + \delta}{2\delta} \approx 0.4203 \in (0, 1)$, implying that the trajectory would keep on moving in the non-smooth boundary to form the quiescent state QS_{s1} via the sliding motion.

With further decrease of the external excitation w , at the point $P_3(w_3, x_3) = (-0.4000, 0)$ corresponding to the point $P_{s0}(x_{s0}, y_{s0}) = (0, 0)$ in the phase portrait Fig 1(a), the auxiliary parameter $q = 0$ passes through minimum value of the interval $(0, 1)$ leading to that the trajectory escapes away from Σ and enters into the smooth region D_- . Consequently, the quiescent state QS_{s1} ends.

Furthermore, according to the equilibrium equation (2), the stable focus-type equilibrium $EQ = (x_0, 0, -x_0)$ in the branch $EB_{\mp 3}$ may have the limitation form:

$$\lim_{x_0 \rightarrow 0} EB_{\mp 3}(w, x) = P_{3,6}(w_{3,6}, x_{3,6}) = (\mp 0.4000, 0) \quad (10)$$

i.e., the trajectory connects with the non-smooth boundary at the stable equilibrium point $P_3(w_3, x_3) = (-0.4000, 0)$.

Now that the stable focus-type equilibrium branch EB_{-3} immediately appears when the trajectory enters into the smooth region D_- at the point P_3 , causing that the trajectory may turn to strictly move along with the stable equilibrium branch EB_{-3} to form the quiescent state QS_{-2} until it arrives at another fold bifurcation point FB_{-2} . Then, the stable equilibrium branch EB_{-3} collides with the unstable equilibrium branch EB_{-2} and disappears together and jumping phenomenon occurs once again, causing the trajectory to jump towards to the stable equilibrium branch EB_{-1} to form the spiking state SP_{-2} till it converges onto the stable equilibrium branch EB_{-1} . Hereafter, the trajectory may stay in the quiescent state QS_{-1} and strictly move along with EB_{-1} till the external excitation reaches its minimum value $w = -1.200$ at the point P_4 . And then, the trajectory turns around to keep on moving with gradually increasing external excitation.

Considering the symmetrical characteristic of the whole system, the rest evolution process of the trajectory from P_4 to P_1 may be similar to the one from P_1 to P_4 till it returns back to the starting point P_1 . Thus, one periodic bursting oscillation is finished.

From above analyses, one may find that the periodic bursting oscillation consists of six quiescent states and four spiking states. In the two smooth regions, the four fold bifurcations $FB_{\pm i} (i = 1, 2)$ may cause the transitions from quiescent states to spiking states, i.e., the quiescent states $QS_{\pm 1}$ connect with the spiking states $SP_{\pm 1}$ via the two fold bifurcations $FB_{\pm 1}$, while the rest two fold bifurcations $FB_{\pm 2}$ connect the quiescent states $QS_{\pm 2}$ with the spiking states $SP_{\pm 2}$. In the non-smooth boundary, the special influence caused by the non-smooth property make a great contribution to the structure of the bursting oscillation as well as the mechanism, which is mainly reflected in two aspects, one is the two non-smooth transitions from the spiking state $SP_{\pm 1}$ to the quiescent state $QS_{s1,2}$, caused by sliding motion; the other is the two non-smooth connections between the quiescent state $QS_{s1,2}$ and the quiescent state $QS_{\mp 2}$.

It can be found that the spiking states may be induced by the jumping phenomenon via fold bifurcations, but there is no related bifurcations corresponding to the transitions from spiking states to quiescent states, leading to that it may be very difficult to classify such non-smooth bursting oscillation by employing the bifurcations connected SP_s with QS_s . And moreover, in the non-smooth boundary, there is no obvious spiking state when the trajectory switches to quiescent states $QS_{\mp 2}$ from quiescent states $QS_{s1,2}$ in such bursting oscillation.

Therefore, with respect to the transitions between SP_s and QS_s , to emphasizing the influence of non-smooth evolutions in the bursting oscillation, the movement in Fig1 can be classified as symmetric focus-focus-sliding motion type non-smooth bursting oscillation via fold bifurcation abutment.

4.2 Non-smooth bursting oscillation with crossing-returning-sliding-escaping motion

Decreasing the value of the parameter to $\beta = -2.200$, it is found that the periodic bursting oscillation in fig3(a) is obviously different from that in fig1(a) near the non-smooth boundary. Fig3(a) and its local enlarged drawing Fig3(b) show that, when the trajectory comes into contact with the non-smooth boundary from the two smooth regions D_{\pm} , two more non-smooth connection points denoted by P_{s1} and P_{s3} appear, at which the trajectory may pass through the non-smooth boundary from one smooth region to the other one directly. Thereafter, the trajectory may return back to the

non-smooth boundary at the two points P_{s2} and P_{s4} respectively soon and stay in the Σ for a while, behaving sliding motion, until it escapes away from the non-smooth boundary at the point P_{s0} to keep on evolving in the related smooth regions. While the rest of the oscillation is similar to the one of $\beta = -1.900$. The details can also be demonstrated by the time history shown in Fig3(c) as well as the locally enlarged drawings Fig3(d1),(d2).

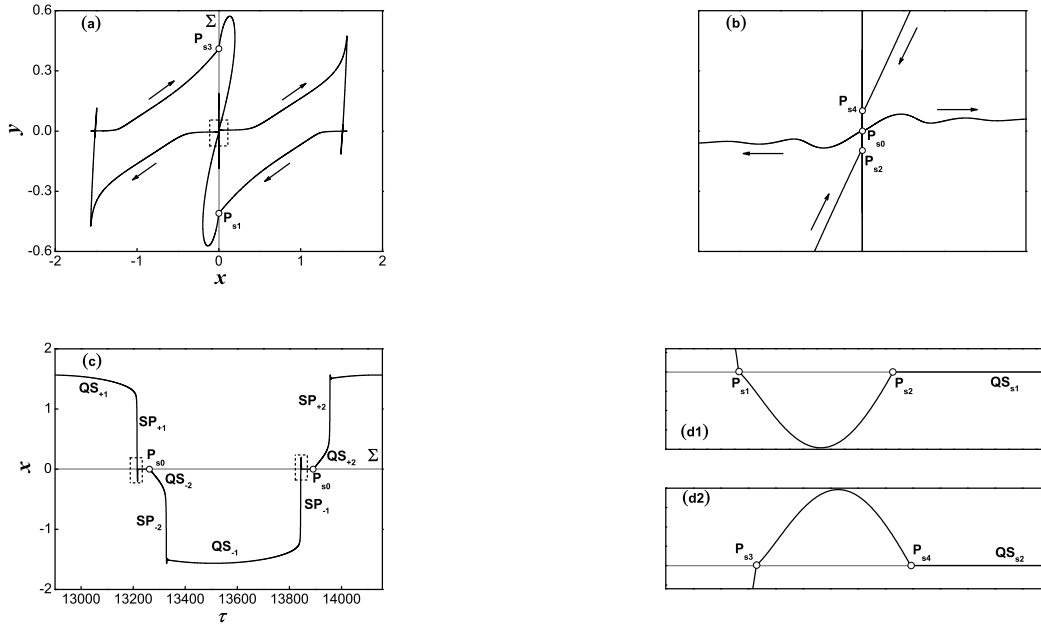


Figure 3: bursting oscillation with $\beta = -2.200$. (a) phase portrait; (b) local enlarged drawing of the phase portrait ;(c)time history;(d1),(d2)locally enlarged drawings of time history.

Fig4(a) gives the equilibrium branches as well as the related bifurcations, which is similar to the structure indicated in Fig2(a). However, after calculations, the coordinates of the four fold bifurcation points $FB_{\pm 1}$ and $FB_{\pm 2}$ in Fig4(a) have changed to $FB_{\pm 1}(w, x) = (\mp 0.0915, \pm 1.2091)$ and $FB_{\pm 2}(w, x) = (\pm 0.7099, \pm 0.4337)$, respectively.

The mechanism of such a periodic bursting oscillation can be investigated by employing the overlap of the transformed phase portrait with the equilibrium branches (shown in Fig 4(b),(c),(d)) and related calculations about auxiliary parameter q as well as coordinates of the non-smooth points. Assuming that the trajectory still starts at the point P_1 with the maximum value of the external excitation. It is easy to find that the evolution of the trajectory from P_1 to P_2 may almost be a copy of the corresponding segment in Fig2(b). However, at the point $P_2(w_2, x_2) = (-0.1236, 0)$ corresponding to the point $P_{s1}(x_{s1}, y_{s1}) = (0, -0.4099)$ in Fig3(a), the auxiliary parameter $q = \frac{-y_{s1} - w_2 + \delta}{2\delta} \approx -0.1669$ is less than the lower bound of the interval $(0, 1)$, implying that the trajectory may pass through the non-smooth boundary directly and enter into the smooth region D_- (shown in Fig4(c)). After a short while, the trajectory returns back to the non-smooth boundary once again at the point $P_3(w_3, x_3) = (-0.1404, 0)$ corresponding to the point $P_{s2}(x_{s2}, y_{s2}) = (0, -0.0069)$ in Fig3(b). At the point P_{s2} , the auxiliary parameter can be computed as $q \approx 0.3159$ which belongs to the interval $(0, 1)$, indicating that the trajectory may exit the spiking state SP_{+1} to keep on sliding within the non-smooth boundary, leading to the quiescent state QS_{s1} , till the external excitation is further reduced to $w = -0.400$.

For the same reason in the condition $\beta = -1.900$, the point $P_4(w_4, x_4) = (-0.4000, 0)$ is also located on the the stable equilibrium branch EB_{-3} , so the trajectory may escape away from the quiescent state QS_{s1} lying within the non-smooth boundary to behave the quiescent state QS_{-2} via moving strictly along with the stable equilibrium branch EB_{-3} until it meets another fold bifurcation point FB_{-2} . Then, the trajectory may behave the spiking state SP_{-2} via the jumping phenomenon caused by the fold bifurcation point FB_{-2} and move towards the stable equilibrium branch EB_{-1} till it converges onto EB_{-1} at last.

Then, the trajectory keeps on moving strictly along with the stable equilibrium branch EB_{-1} , corresponding to new quiescent state QS_{-1} , till the external excitation reaches its minimum value $w = -1.200$ at the point P_5 . And then, the trajectory turns around to keep on moving with gradually increasing external excitation. Still considering the symmetrical

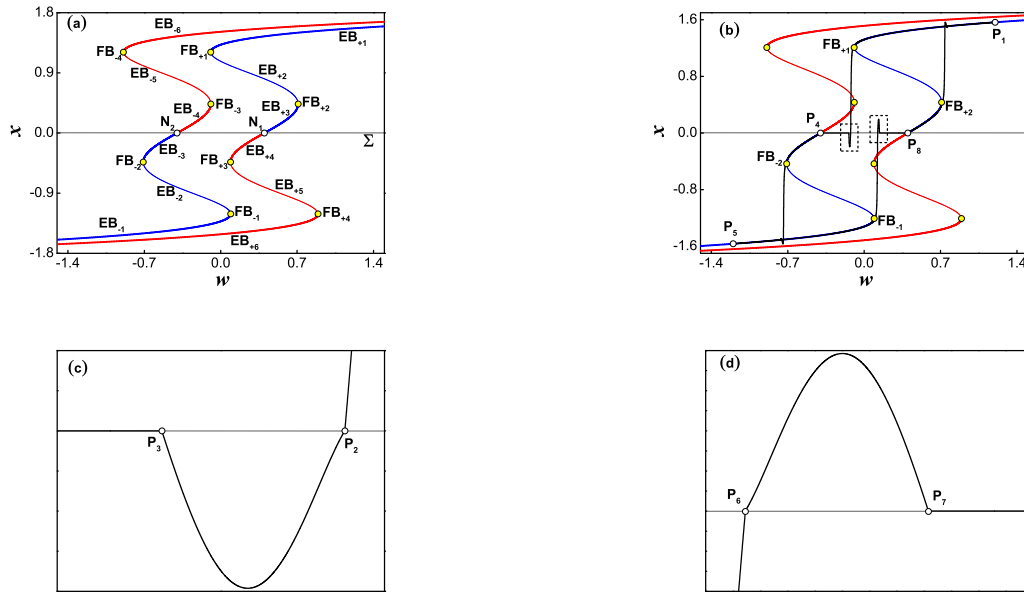


Figure 4: bursting oscillation with $\beta = -2.200$. (a) equilibrium branches of the two smooth subsystems; (b) overlap of transformed phase portrait and equilibrium branches; (c), (d) locally enlarged drawings corresponding to the regions in (b), respectively.

characteristic of the whole system, the trajectory from P_5 to P_1 may repeat the similar evolution on the segment from P_1 to P_5 till it returns back to the starting point P_1 . Thus, one periodic bursting oscillation is finished.

Based on the above analyses, it can be found that the trajectory staying within spiking states $SP_{\pm 1}$ may pass through the non-smooth boundary from one smooth region to the other, and then returns back to behave the quiescent states lying within the non-smooth boundary. As a result, the movement in Fig3 can be classified as symmetric focus-focus-crossing-returning-sliding motion type non-smooth bursting oscillation via fold bifurcations abutment.

4.3 Non-smooth bursting oscillation with crossing motion

When the parameter is further decreased to $\beta = -2.500$, a relatively simple periodic bursting oscillation connected with the two points $P_{s1,2}$ located on the non-smooth boundary can be obtained (shown in Fig5(a)), in which only two quiescent states $QS_{\pm 1}$ located in the smooth regions and two spiking states $SP_{1,2}$ intersecting with the non-smooth boundary exist in one periodic oscillation (shown in Fig5(b)).

From Fig5(c), the equilibrium branches as well as the related bifurcations, one may find that the four fold bifurcation points, computed as $FB_{\pm 1}(w, x) = (\mp 0.6929, \pm 1.3094)$ and $FB_{\pm 2}(w, x) = (\pm 0.6882, \pm 0.4005)$, have a further deviation with the decreasing of the parameter β . The transformed phase portrait overlapped with equilibrium branches as well as the related bifurcations shown in Fig 4.5(d) still can be used to reveal the mechanism of such bursting oscillation.

Corresponding to the phenomena in the first two cases, the mechanism of such bursting oscillation can be analyzed as below in brief. As shown in Fig5(d), the trajectory almost moves along with the stable focus-type equilibrium branches $EB_{\pm 1}$ with the variation of the external excitation, performing the two quiescent states $QS_{\pm 1}$ till it meets the two fold bifurcation points $FB_{\pm 1}$ located on the real equilibrium branches. Then, jumping phenomenon caused by the fold bifurcations occurs, leading to that the trajectory may move towards to the non-smooth boundary, displaying the two spiking states $SP_{1,2}$. When the trajectory comes into contact with the non-smooth boundary at the two points $P_{2,4}$ corresponding to the two points $P_{s1,2}$ in the phase portrait Fig5(a), the auxiliary parameter values, computed as $q \approx -0.8857$ and $q \approx 1.8857$, respectively, are not in the interval $(0, 1)$, indicating that the trajectory may pass through the non-smooth boundary to enter into the opposite smooth region directly till the trajectory converges onto the sole stable focus-type equilibrium branches $EB_{\pm 1}$, performing the quiescent states once again.

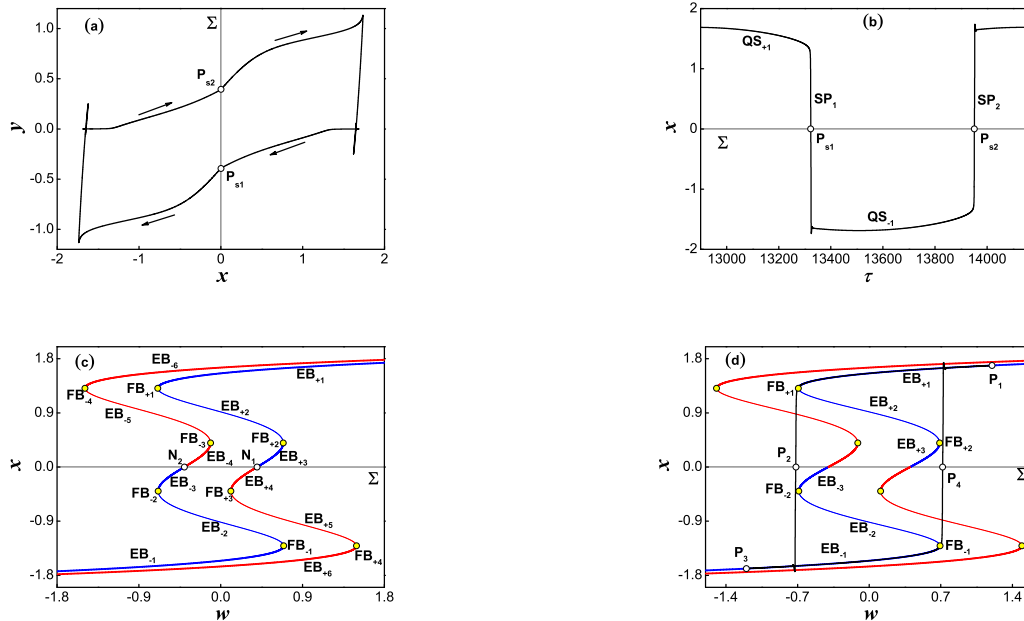


Figure 5: bursting oscillation with $\beta = -2.500$. (a) phase portrait; (b) time history; (c) equilibrium branches of the two smooth subsystems; (d) overlap of the transformed phase portrait and equilibrium branches.

By drawing the experience from the classification methods mentioned in the two previous periodic bursting oscillations, such periodic bursting oscillation in Fig5(a) can be classified as focus-focus type non-smooth bursting oscillation via fold bifurcation abutment.

Note that two quiescent states caused by the sliding motion may be observed on the non-smooth boundary in the two previous bursting oscillations except for the third one. The reason is that, with the decreasing of the parameter value, the external excitation values corresponding to the two fold bifurcation points $FB_{\pm 1}$ may be out of the closed interval $[-|\delta|, |\delta|]$ determined by the non-smooth term. So the trajectory has no opportunity to enter into the non-smooth boundary to form the two quiescent states lying within the non-smooth boundary. As a consequence, the third type bursting oscillation may be four quiescent states less than the two previous ones.

5 Conclusions

For a Filippov-type system involving an external excitation, when an order gap exists between the exciting frequency and the natural frequency, three different non-smooth periodic bursting oscillations, distinguished from different non-smooth evolutions when the trajectory comes into contact with the non-smooth boundary, are exhibited with the property parameter conditions in this paper. Since the whole system is divided into two smooth subsystems by the non-smooth boundary, both the equilibrium branches as well as the related bifurcations of each subsystem and the potential non-smooth dynamic behaviors are analyzed to reveal the mechanism as well as the classification of such non-smooth bursting oscillations. It is found that the transition from quiescent states to spiking states can be mainly induced by jumping phenomena caused by fold bifurcations. However, the transition from spiking state to quiescent state includes two different paths, one is that the trajectory can converge onto the stable equilibrium branch; the other is that the trajectory can enter into the sliding motion lying within the non-smooth boundary. In another word, two obviously different incentives to quiescent states can be observed from the bursting oscillations, one is the stable equilibrium branch; the other is the non-smooth property on the non-smooth boundary.

References

- [1] W. Teka, R. U and A. Mondal. Spiking and bursting patterns of fractional-order Izhikevich model. *Communications in Nonlinear Science and Numerical Simulation*, 56(2018): 161–176.
- [2] H. GU. Experimental observation of transition from chaotic bursting to chaotic spiking in a neural pacemaker chaos. *Chaos*, 23(2)(2013): 023126.
- [3] P. Gifani and J. Goncalves. Biexcitability and bursting mechanisms in neural and genetic circuits. *IFAC Proceedings Volumes (IFAC-PapersOnline)*, doi: 10.3182/20140824-6-ZA-1003.02630.
- [4] Y. Yu, Z. Zhang and X. Han. Periodic or chaotic bursting dynamics via delayed pitchfork bifurcation in a slow-varying controlled system. *Communications in Nonlinear Science and Numerical Simulation*, 56(2018): 380–391.
- [5] Q. Bi, R. Zhang and Z. Zhang. Bifurcation mechanism of bursting oscillations in parametrically excited dynamical system. *Applied Mathematics and Computation*, 243(2014): 482–491.
- [6] V. Bykov and V. Gol'dshtein. Fast and slow invariant manifolds in chemical kinetics. *Computers & Mathematics with Applications*, 65(10)(2013): 1502–1515.
- [7] G. Chumakov, N. Chumakova and E. Lashina. Modeling the complex dynamics of heterogeneous catalytic reactions with fast, intermediate, and slow variables. *Chemical Engineering Journal*, 282(2015): 11–19.
- [8] J. Rinzel. Bursting oscillations in an excitable membrane model. In: Sleeman B, Jarvis R, editors, *Ordinary and Partial Differential Equations*, 304–316. Springer-Verlag, New York. 2006.
- [9] Izhikevich and M. Eugene. Neural excitability, spiking and bursting. *International Journal of Bifurcation and Chaos*, 10(6)(2000): 1171–1266.
- [10] X. Chen, S. Li, Z. Zhang and Q. Bi. Relaxation oscillations induced by an order gap between exciting frequency and natural frequency. *Science China(Technological Sciences)*, 60(2017): 289–298.
- [11] X. Han, ed. Fast-slow analysis for parametrically and externally excited systems with two slow rationally related excitation frequencies. *Physical Review E*, 92(1–1)(2015): 012911.
- [12] Z. Zhang, B. Liu and Q. Bi. Non-smooth bifurcations on the bursting oscillations in a dynamic system with two timescales. *Nonlinear Dynamics*, 79(2015): 195–203.
- [13] H. Simo and P. Woafu. Bursting oscillations in electromechanical systems. *Mechanics Research Communications*, 38(8)(2011): 537–541.
- [14] S. Adly. Attractivity theory for second order non-smooth dynamical systems with application to dry friction. *Journal of Mathematical Analysis and Applications*, 322(2)(2006): 1055–1070.
- [15] J. Fan, S. Xue and S. Li. Analysis of dynamical behaviors of a friction-induced oscillator with switching control law. *Chaos, Solitons & Fractals*, 103(2017): 513–531.
- [16] T. Specker, M. Buchholz and K. Dietmayer. A New Approach of dynamic friction modelling for simulation and observation. *IFAC Proceedings Volumes (IFAC-PapersOnline)*, 19(2014): 4523–4528.
- [17] F. Diekert. Threatening Thresholds? The effect of disastrous regime shifts on the non-cooperative use of environmental goods and services. *Journal of Public Economics*, 147(2017): 30–49.
- [18] M. Han, C. Zhao, G. Feng and F. Shi. Bayesian inference of the groundwater depth threshold in a vegetation dynamic model: A case study, lower reach, Tarim River. *Quaternary International*, 380–381(2015): 207–215.
- [19] X. Li, D. Zhang, F. Zhang and P. Zhang. The eco-hydrological threshold for evaluating the stability of sand-binding vegetation in different climatic zones. *Ecological Indicators*, 83(2017): 404–415.
- [20] R. Rocha, J. Ruthiramoorthy and T. Kathamuthu. Memristive oscillator based on chuas circuit: stability analysis and hidden dynamics. *Nonlinear Dynamics*, 88(2017): 2577–2587.
- [21] R. Leine and D. Campen. Bifurcation phenomena in non-smooth dynamical systems. *European Journal of Mechanics - A/Solids*, 25(4)(2006): 595–616.